

High Force Density Textile Electrostatic Clutch

Ronan Hinchet and Herbert Shea*

Clutches are key elements for blocking or coupling motion in wearable systems such as soft exoskeletons, haptic clothing, and rehabilitation equipment. Electrostatic clutches (ESclutches) are compact and light, making them particularly well-suited for wearable applications. They are variable capacitors whose electrodes can slide with respect to each other, with a frictional force between electrodes proportional to the square of the applied voltage. A high force-density textile-based ESclutch is reported here, generating frictional shear stresses of 21 N cm^{-2} at only 300 V, a stress level 11 times higher than any other ESclutch, and 88 times better than textile-based ESclutches. Actuation and release time are inferior to 5 and 15 ms. Power consumption is below 1.2 mW cm^{-2} . To reach such high frictional stresses, a dielectric material with high permittivity is chosen (P(VDF-TrFE-CTFE)), a fabrication process that enables highly planar dielectric and conductive films on textile is developed, and an alternating current waveform is optimized to minimize space charge. The ESclutch is thin, highly flexible, and weighs only 30 mg cm^{-2} . The device demonstrated here is designed for wearable applications such as kinesthetic haptic feedback for virtual reality or for soft exoskeletons.

Clutches are essential components of many robotic systems, dynamically blocking or coupling a wide range of motion types, and enabling variable stiffness systems. While much research on soft robotics^[1–4] has centered on actuators,^[5] soft clutches are poised to play an important role in wearable systems such as soft exoskeletons,^[6–8] gloves for virtual reality (VR),^[9–11] or rehabilitation equipment^[12–15] where there is a need for a flexible and low-power means to block motion, or to actively link or unlink compliant elements.

Numerous types of clutches have been developed,^[16] most of them based on rigid materials. Pneumatic vacuum jamming clutches can be soft, but require tubes, pumps and valves to control them. From a control perspective, electrically-driven clutches are well matched to robotic and haptic applications. Electromagnetic clutches are effective, but are bulky and have high power consumption. Power consumption can be reduced by using mechanical latches, at the expense of reduced speed and increased complexity. Magnetorheological fluid designs are simpler but heavier.^[17–19] The aforementioned clutches are

not well suited to wearable applications given the lack of compliance and high mass. Piezoelectric based clutches^[20] are lighter and consume less power. They can generate high forces, but are complex and rigid. Electrostatic clutches^[8,9,21–24] (ESclutches) can be compact, light, low profile and flexible, making them well suited to wearable applications.


Electrostatic (ES) clutches were first reported in 1923^[25] and found little use until the 1990s.^[26,27] They are variable capacitors whose electrodes can slide with respect to each other, while maintaining a roughly constant out-of-plane spacing. The friction between the electrodes is to first order proportional to the electrostatic attraction between them, generated by the applied voltage difference across the dielectric material separating the electrodes (Figure 1A,B). It is thus possible to electrically tune the friction force. Once the capacitor is charged, the power consumption is extremely low (typically less than

$1 \mu\text{W}$, due only to small leakage current through the dielectric).

Electrostatic clutches and switches have been investigated at the microscale.^[28–31] Progress in high-permittivity materials and wider availability of conductive textiles have led to a revival of research in macroscale ESclutches, in configurations that are compatible with soft or wearable robotics applications. Diller et al.^[8,21] developed ESclutches for exoskeleton actuation with friction shear stress of up to 1.25 N cm^{-2} and release time below 30 ms. ESclutches have been used as well for kinesthetic haptic feedback to block fingers motion^[9] with friction shear stress up to 1.95 N cm^{-2} . Ramachandran et al.^[22] integrated ESclutches on textile with stress up to 0.24 N cm^{-2} . Stacking ESclutches also enabled rendering variable stiffness^[23,32] systems. Finally, a geometry very similar to ESclutches takes advantage of an electrostatic zipping phenomena to generate large displacements.^[33]

While the basic concept of an ESclutch is straightforward (Figure 1A,B), designing an effective mechanism for wearable applications is not. The device must generate high blocking forces (ideally of order 100 N cm^{-2}) while engaging and disengaging in milliseconds. The device needs to be mm-thin, highly flexible and lightweight. Textile substrates therefore seem like the obvious choice, but devices reported to date have important limitations. First, the frictional shear stress has been below 1 N cm^{-2} . A higher force density is needed for many applications. Second, many ESclutches require drive voltages of order 500 V or higher. Third, textile integration is a must for comfortable, light weight and highly flexible devices in a thin form factor.

Dr. R. Hinchet, Prof. H. Shea
Ecole Polytechnique Fédérale de Lausanne (EPFL)
Soft Transducers Lab (LMTS)
71b rue de la Maladière 2002, Neuchâtel, Switzerland
E-mail: herbert.shea@epfl.ch

 The ORCID identification number(s) for the author(s) of this article can be found under <https://doi.org/10.1002/admt.201900895>.

DOI: 10.1002/admt.201900895

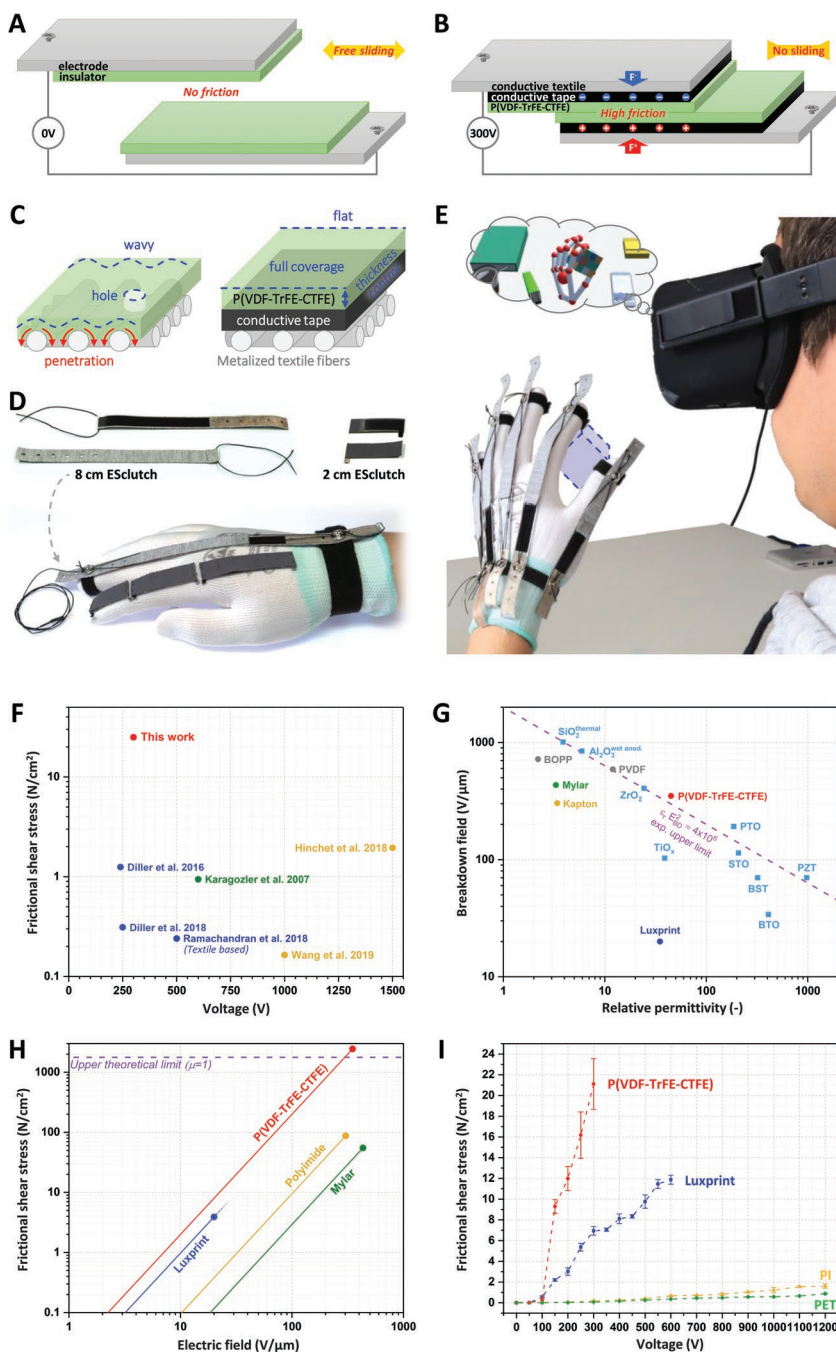


Figure 1. A) Schematic view of an ESclutch free to slide with 0 V applied between the electrodes. B) Schematic view of a textile ESclutch in the blocking state with 300 V applied between the electrodes, pulling both sides together. C) Schematic drawing of a textile substrate with a thin dielectric layer coated directly on it, leaving holes in the insulating layer (left), and with a dielectric film attached to the textile using a thin smooth conductive adhesive, leading to a much more uniform insulator layer (right). D) Photograph of both halves of 8-cm and 2-cm long textile ESclutches, and complete ESclutches mounted on a glove to block either entire finger motion or only individual joints. E) Photo of a kinesthetic haptic feedback glove based on integrated textile ESclutches, illustrating a VR application (virtual objects feel solid by rapidly blocking finger motion when virtual contact is detected). F) Comparison of the friction shear stress generated by different ESclutch devices from literature,^[8,9,21–24] showing the very high frictional shear stress from our textile ESclutch. G) Breakdown voltage versus relative permittivity for selected dielectric materials. Blue indicates ceramics. Other colors indicate polymers. Data are given in Table S1 (Supporting Information). H) Computed frictional shear stress versus electric field for ESclutches using different dielectric materials. Data are given in Table S2 (Supporting Information). I) Measured frictional shear stress versus applied voltage on textile base ESclutches showing the higher stress reached by P(VDF-TrFE-CTFE) based ESclutches compared to others different dielectric polymers. Dielectric film thickness is 12.5 μm .

A high-force density textile-based ESclutch is reported here that addresses the three key challenges mentioned above. Our ESclutch generates frictional shear stress up to 21 N cm^{-2} at a voltage of only 300 V and with actuation and release time inferior to 5 and 15 ms. It is highly flexible, ultralight (less than 1.1 g for an integrated device that blocks one finger) and is less than 2 mm thick. The device demonstrated here is designed for wearable applications such as kinesthetic haptic feedback gloves (Figure 1D) for virtual reality (Figure 1E) or for soft exoskeletons. The clutch is comfortable, washable and it can be readily adapted to different body shapes.

To reach frictional shear stress 11 times higher than reported in the literature^[9] (Figure 1F), i) dielectric material with very high permittivity were chosen (poly vinylidene fluoride, trifluoroethylene, 1,1-chlorotrifluoroethylene (P(VDF-TrFE-CTFE))), ii) a fabrication process that enables highly planar dielectric and conductive films on knitted or woven textile was developed that in addition is a reliable self-clearing design resilient to short circuits, and iii) an Alternating Current (AC) waveform was optimized to minimize space charge accumulation in dielectrics to obtain high force density while being able to rapidly disengage the ES clutch.

The ESclutches consist of two flexible and partially overlapping electrodes separated by a thin insulator, and possibly by an air gap. The electrodes can slide with respect to each other (Figure 1A). When the voltage difference between the electrodes is zero, there is no electrostatic attraction between the electrode, and they slide freely. When a voltage is applied between the electrodes (Figure 1B), electrostatic attraction pulls them together. This electrically-controlled normal force increases the sliding (or shear) frictional forces between the strips, impeding or fully blocking the sliding motion. Electrodes could be for instance thin steel shim, or metallized mylar, or conductive fabric.

A simple model based on electrostatic attraction and dry Coulomb friction is widely used for ESclutches. The conductivity of

shear stress versus electric field for ESclutches using different dielectric materials. Data are given in Table S2 (Supporting Information). I) Measured frictional shear stress versus applied voltage on textile base ESclutches showing the higher stress reached by P(VDF-TrFE-CTFE) based ESclutches compared to others different dielectric polymers. Dielectric film thickness is 12.5 μm .

the thin insulator layer used here is effectively zero, leading to no Johnsen-Rahbek effect.^[34,35] For ideal parallel plate capacitances,^[24,36,37] the normal electrostatic attraction between two ESlutch strips is given by

$$F_N = \frac{\epsilon_0 A \epsilon_r V^2}{2 d^2} = \frac{\epsilon_0 A}{2} \epsilon_r E^2 \quad (1)$$

where A is the overlap area, ϵ_0 is the vacuum permittivity, ϵ_r is the relative permittivity of the insulator, V the applied voltage, d the distance between the electrodes and E the applied electric field. The higher the applied voltage, the higher the compression force. Maximizing the ESlutch's friction stress requires maximizing the compression force F_N which, for a given insulating material, depend on its breakdown electric field (E_{bd}) and ϵ_r . Therefore, choosing the dielectric material with the highest ratio $E_{bd}^2 \times \epsilon_r$ is key to high clutch performance.

An empirical maximum limit has been reported for the product $E_{bd}^2 \times \epsilon_r$ ^[38,39] (dashed line in Figure 1G). The frictional force between the ESlutch's electrodes is, to first order, the product of the electrostatic force F_N and the static friction coefficient μ . The maximum achievable friction force for an ES clutch is

$$F_{Fmax} = \mu \times F_{Nmax} = \frac{\epsilon_0 A}{2} \times \mu \epsilon_r E_{bd}^2 \quad (2)$$

The frictional force is linearly proportional to the overlap area A . Therefore, the frictional shear stress was used to compare results. It is the tangential force per unit of area generated on a surface by friction. It is equal to

$$P_{ss} = \frac{\epsilon_0}{2} \times \mu \epsilon_r E^2 \quad (3)$$

For the limiting case of $\mu = 1$, the theoretical maximum frictional shear stress for an ESlutch is 1770 N cm^{-2} operating at the empirical maximum limit for $E_{bd}^2 \times \epsilon_r$.

Figure 1G plots breakdown voltage versus relative permittivity for several dielectric oxide ceramics and polymers, to aid in identifying the best insulator for ESlutches. The best materials in terms electrostatic force are located on the top right of the plot, with high permittivity and breakdown field. For wearable applications the devices must be highly flexible, so we focused on polymers rather than ceramics, accepting a slight reduction in force. Slippery polymers such as PTFE^[40] are to be avoided; materials with high μ are preferred.

Figure 1H plots the maximum theoretical frictional shear stress versus electric field (Equation (3)) for four polymers (Tables S1 and S2 and Figure S1, Supporting Information), helping to identify promising polymers. Using P(VDF-TrFE-CTFE) is predicted to generate higher frictional shear stress than Luxprint, Kapton and Mylar for any given electric field. This enables using lower voltages to reach a given force, or using a smaller surface for a given force and voltage. Using lower voltages simplifies the design of electrical insulation, and the control electronics are easier to design and much lower cost.

The model described above assumes perfectly flat and parallel electrodes. While this was the case for our earlier work using thin steel shim as the electrodes,^[9] it is not generally the case when using metalized textile as the electrodes. In our initial experiments, the measured frictional shear stress generated by

devices for which P(VDF-TrFE-CTFE) was directly coated on the textile electrodes (Figure 1C) was low, less than 1 N cm^{-2} . The device had a low capacitance of 19 pF cm^{-2} . Textile electrodes often lead to low capacitance because of their 3D knitted structure, which creates high roughness and holes in the woven electrode (Figure S2, Supporting Information). A low capacitance leads to low electrostatic force, hence low frictional shear stress. Further complicating matters, textile electrodes are also hard to uniformly coat (Figure 1C).

To solve this poor coating, we first covered the textile with $31.7 \text{ }\mu\text{m}$ thick conductive tape (ARcare 90366 from Adhesive Research) to planarize it. We then attached the $25 \text{ }\mu\text{m}$ thick dielectric films, that were prepared in a separate casting process (see experimental section). This method increased the capacitance of the device by over 8 times to 156 pF cm^{-2} and generated much higher friction shear stresses. The conductive tape also made it easier to control the thickness of the dielectric thin film because the tape is flat whereas the textile has roughness and holes on a $10\text{--}100 \text{ }\mu\text{m}$ scale (Figure 1C). This approach is electrically self-clearing, with electrodes highly resilient to short circuits.

We tested four polymers (Figure 1I): P(VDF-TrFE-CTFE) because it has a very high permittivity of 45; Luxprint has a high permittivity of 35 and is used in the clutch literature; Kapton has a high dielectric breakdown but a low permittivity of 3.4, and it has been used previously for haptic feedback gloves;^[9] PET because it is similar to Kapton ($\epsilon_r = 3.3$) but much cheaper and very easily sourced.

Operating at electric fields close to the electrical breakdown should give the highest forces. Decreasing the dielectric layer thickness should enable high forces at low voltage. However, for ease of manipulation, for reliability and durability purposes, the dielectric layer should not be too thin. We therefore choose to fabricate dielectric layers from 12.5 to $25 \text{ }\mu\text{m}$ thick. This thickness gives sufficient electrical and mechanical robustness while remaining relatively easy to fabricate and to handle. Moreover, at such thickness and below 350 V , this system is self-clearing for electrical short circuits.^[41–43] When a short circuit occurs through the P(VDF-TrFE-CTFE), it evaporates, leaving a small hole. Given the Paschen curve, air cannot sustain an electrically breakdown below 350 V for this gap spacing.^[44–46] This situation also holds if the hole is due to an initial defect or occurs due to wear.

To characterize clutch performance, we attached two strips facing each other on a commercial pull tester. To measure the shear friction force, we pulled one strip at constant speed while recording the required applied force. Figure 1I shows that P(VDF-TrFE-CTFE) gives the best performance of all polymers we studied. Frictional shear stress reaches 21 N cm^{-2} at only 300 V . This is 11 times higher than previous best results obtained with Kapton at 1500 V .^[9] Kapton devices provide a frictional shear stress of 1.6 N cm^{-2} at 1200 V . These numbers are in agreement with our previous work.^[9] PET reached only 0.9 N cm^{-2} at 1200 V . Lastly, Luxprint is a promising material, reaching frictional shear stress up to 12 N cm^{-2} at 600 V . This value is much higher than reached in previous studies^[8,21,22] probably because of the optimized process reported here using thin conductive tape to planarize the fabric. According to the model given in Equation (3), the frictional shear stress should

be proportional to the square of the electric field.^[21,37] The shear stress measured on Kapton- and PET-based devices are proportional to the voltage to the power 2.02 and 1.97. This agrees very well with theory. Similarly, below 8 N cm⁻² (for voltages below 400 V), the shear stress measured on devices based on 25 µm thick P(VDF-TrFE-CTFE) layers (Figure S3, Supporting Information) was proportional to the voltage to the power 1.92. Devices based on thinner 12.5 µm thin P(VDF-TrFE-CTFE) and Luxprint layers generated much higher shear stresses. However, their shear stress was proportional to the voltage to the power 1.19 and 1.15, rather than the theoretical value of 2. One explanation for this could be a transition to a different friction model at very high shear stresses. Another explanation could be a reduction in permittivity at very high fields. Other possible phenomena include Van der Waals interactions, stiction effects and geometric confinement.^[37,47,48]

We investigated lifetime and failure modes by subjecting our textile ESlutches to pulling forces exceeding their maximum holding friction force and thus generating numerous consecutive stick-slip sequences (Figure 2A) at different voltages. Below 300 V, the 12.5 µm thick P(VDF-TrFE-CTFE) layer did not show any permanent electrical failure thanks to the self-clearing design. After a hundred of stick-slip events under high shear stress, the P(VDF-TrFE-CTFE) layer started to wear out, leading to a decreasing friction stress (Figure S4, Supporting Information). This is mostly due to the characterization process that pushes the ESlutch past its limit to measure its maximum blocking force just before slipping. In most planned applications, the ESlutch is designed to block forces without slipping, leading to much lower wear out. We also noted some deterioration: above ≈10 N cm⁻², wrinkles of the tape and the P(VDF-TrFE-CTFE) layers started to appear on few devices. In addition, at ≈20 N cm⁻², the adhesive started to locally delaminate from the textile, leading to a decrease in the frictional shear stress over time. While we can generate even higher shear stresses by applying more than 300 V across the P(VDF-TrFE-CTFE) films, the mechanical force was too high for the adhesive and dielectric films, and the devices degraded after tens of stick-slip. Some textile substrates even ruptured, showing the frictional shear force can be higher than the rupture force of the textile. Luxprint devices performed well until 600 V. However, in comparison to P(VDF-TrFE-CTFE) which is elastic resilient and ductile, Luxprint is brittle and cracks easily under high loads. As a consequence, at voltages higher than 600 V, when the ESlutch textile substrate started to stretch, the Luxprint layer started to crack and short circuits appeared (Figure S5, Supporting Information) leading to device failure.

Actuating an ESlutch requires applying high electric fields, that can lead to the accumulation of space charge in the dielectric layer.^[49–52] For ESlutches, space charge has 2 detrimental effects. First, when the ESlutch is engaged, it screens the voltage applied between the electrodes, decreasing the electrostatic attraction between the electrodes and therefore the friction force (Figure 2B). Secondly, when the ESlutch is disengaged and no voltage is applied, it generates electrostatic attraction between the two dielectric layers which increases the friction force (Figure 2C). Because space charge builds up with time and with cycles (until a saturation level), and can persist for minutes or even hours depending on dielectrics;^[53]

the longer the voltage is applied between ESlutch's electrodes, the more the space charge increases, and therefore, the more the “on-state” friction force decreases and the “off-state” friction force increases. The higher the drive voltage, the stronger these effects are.

One documented method to reduce space charges is to periodically reverse the voltage polarity. We implemented this polarity reversal using a unipolar Direct Current (DC) power supply coupled with an H-bridge to generate a symmetric bipolar rectangular AC voltage signal. To compare DC and AC actuation, ESlutches were pulled apart at constant speed and the frictional shear stress was recorded (Figure 2A). When engaged at low voltage (100 V), there are few space charges and the force blocked under DC and AC actuation voltages are similar (Figure S6, Supporting Information). At higher voltages (300 V), space charges are more important, and reduce by 5 times the stress generated in DC actuation compared to AC actuation (Figure 2D). AC actuation enables generating much higher frictional shear stress than DC actuation. When disengaged after actuating an ESlutch at high voltage (400 V) for 10 s and then turning the voltage to 0 V, the friction curves (Figure 2E) show a friction peak whose magnitude depends on the force blocked and the dielectric material (Figure S7, Supporting Information). The friction peak is at least 2 times lower after AC actuation compared to after DC actuation. In addition, the peak increases in amplitude and duration after 10 consecutive DC actuations because of the accumulation of space charges, whereas the friction peak remains constant after 10 consecutive AC actuations. AC actuation enables more consistent and much faster release than DC actuation.

Performance with AC actuation is far superior to DC actuation, but requires higher average power because the ESlutch is periodically charged and discharged. The power P can be approximated as the energy required to charge an equivalent capacitor multiplied by the AC frequency f

$$P = \frac{1}{2} CV^2 \times 2f = \frac{\epsilon_r \epsilon_0 f A V^2}{d} \quad (4)$$

For a 12.5 µm thick P(VDF-TrFE-CTFE) based ESlutch of area 1 cm² operated at 300 V at 10 Hz, Equation (3) gives a power consumption of 1.43 mW. We measured a power draw of 1.22 mW, in good agreement (Figure S8, Supporting Information).

The time to actuate the ESlutch is the sum of the time to electrically charge the ESlutch and then to zip the two electrodes together. Zipping (or pull-in) is related to the stiffness of the substrates and to the initial gap between the strips. In our case, the textile strips were very flexible and already in contact, so the zipping time was negligible (ms or shorter). The time it takes to electrically charge the ESlutch depends on the clutch capacitance and on the maximum current the high voltage power supply (HVPS) can source. Considering a power supply with current limited to 1 mA for safety, and a 25 µm thick P(VDF-TrFE-CTFE) based ESlutch of area 3 cm², it should take 3.6 ms to charge the ESlutch to 99% of the intended 300 V. Experiments (Figure 2F) shows that such an ESlutch engaged in less than 5 ms.

The ESlutches were turned off by setting the control voltage to 0 V, hence discharging the capacitor and removing the electrostatic force. This process should in theory be as fast as actuation, but Van Der Waals forces and surface forces can slow

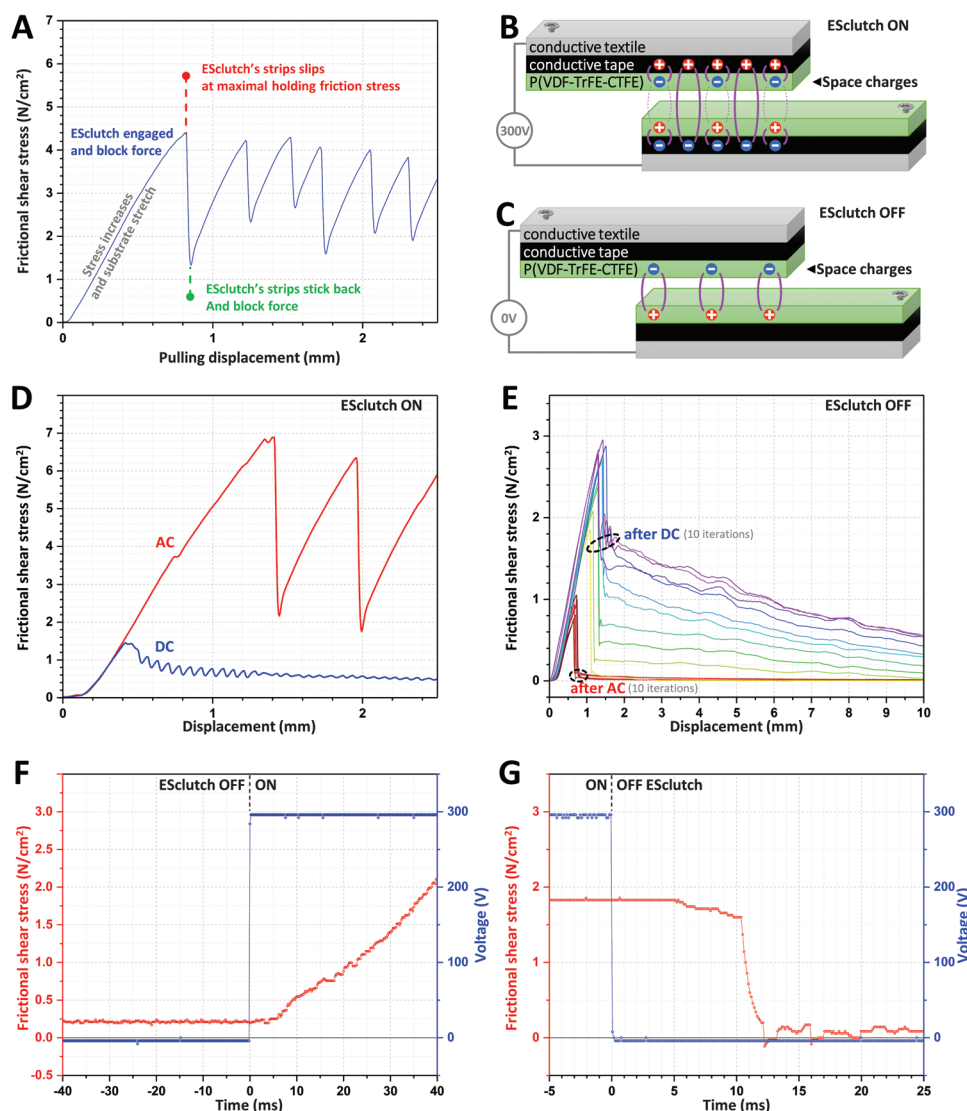


Figure 2. Performance of textile-based clutch with a 25 μm thick P(VDF-TrFE-CTFE) dielectric film A) Frictional shear stress versus applied displacement, generated by pulling one half of a textile ESclutch, operated at 300 V. The friction curve shows 6 stick and slip sequences. B) Schematic illustration of an ESclutch with space charges in the dielectric layers when engaged at 300 V (the trapped charge reduces shear stress) and C) when disengaged at 0 V (the trapped charges lead to an unwanted shear stress). D) Comparison of measured frictional shear stress generated by a textile ESclutch actuated at 300 V in AC actuation at 10 Hz and in DC actuation: the AC actuation leads to much higher shear stress due to lower space charge effects. E) Measured frictional shear stress remaining after the release of a textile ESclutch following 10 s actuation at 400 V in DC, and much lower measured stress after AC actuation at 10 Hz during 10 s. The AC actuation mode used the same DC source coupled with an H-bridge. F) Measured frictional shear stress and voltage bias curves when engaging and G) when disengaging a textile ESclutch in AC actuation mode, showing rapid response of under 5 ms to actuate and 15 ms to release.

down the release. Experimentally, release times between 10 and 15 ms were measured (Figure 2G).

Compared to previous textile based ESclutch^[22] our ESclutch has a frictional shear stress 88 times higher while reducing the voltage from 500 to 300 V. We can block loads of several kg with only few cm² of overlap between strips. For example, a 1 cm² ESclutch can hold a 2 kg load (Figure 3A). The simple structure of the clutch makes it easy to scale it for different applications. With a 10 cm² device, we can block a 20 kg load (Figure 3B). This is a 11 times higher force density compared to best non-textile based ESclutches.^[8] In addition, the ESclutch consumes only 1.22 W cm⁻² and weighs 30 mg cm⁻². As a result,

it has a force/power consumption ratio of 17.2 kN W⁻¹ and a force/mass ratio of 700 kN kg⁻¹ which makes it one of the most efficient electrically driven clutches.^[21] This high performance allows blocking high forces while keeping a reasonable device size, weight and power consumption, making it an excellent choice for exoskeleton and wearable haptic applications.

The textile substrate makes the ESclutch highly flexible, ultra-light and thin which eases comfortable integration in clothes. The ESclutch is washable. Washing it with soapy water during 5 min cleaned the surfaces of the ESclutch and restored most of its performance, removing finger oil and particles generated by wear (Figure 3C).

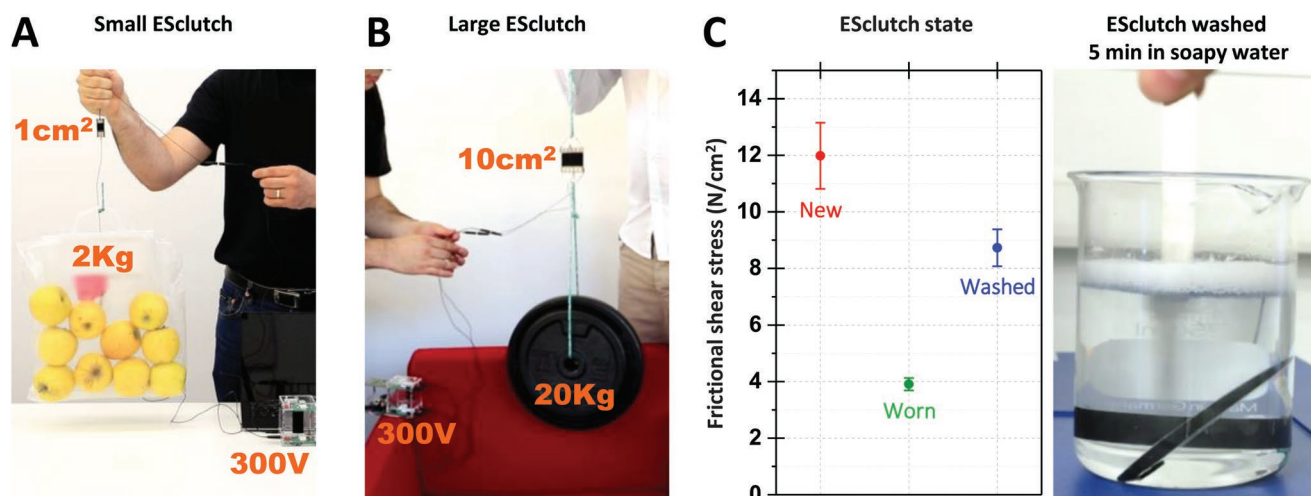


Figure 3. A) Small ESclutch of area 1 cm² holding a 2 kg bag of apples. B) Large ESclutch of area 10 cm² holding a 20 kg weight. C) Frictional shear stress measured at 200 V before and after washing with soapy water a textile ESclutch that was worn for 5 min.

Potential applications are numerous and go well beyond the field of robotics in which clutches are most widely used. Kinesthetic haptic feedback is a field of rapidly growing importance,^[54–57] for instance, in VR, actively blocking a user's fingers' motion to give the user the convincing feeling that virtual objects are solid (Figure S9, Supporting Information). The high force density associated with the textile substrate of ESclutches enables placing them on the hand and on each fingers' joint to block their motion. Thus, it is possible to provide kinesthetic haptic feedback with comfort and taking only as much thickness as a thin glove (Figure 1E). Moreover, because the friction stress depends on the applied voltage, it is possible to generate a feeling of variable stiffness for virtual squishy objects using different drive voltages. This greatly improves immersion and dexterity when manipulating virtual objects, and it enhances interactions in virtual world^[9] which has numerous applications.^[58–60]

The electrostatic clutch presented here generates very high frictional shear stress up to 21 N cm⁻² at 300 V, which is 11 times higher than best ESclutches while consuming only 1.22 mW cm⁻². This enables higher forces and smaller ESclutches than existing devices. In addition, the textile integration allows for ultralight and highly flexible ESclutches which increases comfort and facilitates integration for wearable applications, for instance blocking fingers' motion to provide kinesthetic haptic feedback when grabbing virtual objects. Such blocking mechanism can also be applied on the body for textile-based robots and exoskeletons.

Experimental Section

Materials: Poly (P) vinylidene fluoride (VDF), trifluoroethylene (TrFE), 1,1-chlorotrifluoroethylene (CTFE) powder from Piezotech-Arkema (Piezotech RT-TS, P(VDF-TrFE-CTFE) terpolymer) was diluted at 14 % in Methyl Ethyl Ketone (MEK). Thin films were produced by blade casting using a Zehntner ZAA 2300 film applicator. After casting, P(VDF-TrFE-CTFE) thin films were cured at 102 °C for 2 h. Similarly, Luxprint 8153 polymer-barium titanate ceramic composite from Dupont was cast into thin films and cured at 140 °C for 1 h. The 12.5 μm thick Kapton thin film was purchased from Dupont. The 12.5 μm thick Mylar thin film was cut from a survival blanket from Aptonia. Thin films were transferred using

conductive adhesive, ARcare 90366 from Adhesive Research, onto nickel/copper coated Polyester (PE) ripstop fabric from LessEMF. ESclutches were integrated onto general purpose nylon glove from Eurostat using standard Velcro and rubber string, snap buttons and textile transfer adhesive.

Characterization: A pull-tester (Single Column Universal Testing System) model 3340 from Instron with a 50 N and a 2 kN load cell was used to characterize the ESclutch. A 1 W 1200 V Peta-pico-Voltron^[61] high voltage power supply was used with an H-bridge to actuate the ESclutches. For the fast acquisition of the actuation and release time of ESclutch, a 111 N force sensor from Futek, a TREK model 609E-6 high voltage amplifier with a resistance of 300 kΩ in series, a low frequency generator Agilent 33521A, and an Agilent Technologies DSO1014A oscilloscope was used. For capacitive measurements, we used a Precision LCR meter Agilent E4980A with a Kelvin clip lead Agilent 16089B. The experiments involving human subject have been performed with the full, informed consent of the volunteer.

Supporting Information

Supporting Information is available from the Wiley Online Library or from the author.

Acknowledgements

This work was supported in part by a grant from the Hasler Foundation (Switzerland), Cyber Human Systems program. The authors thank Piezotech-Arkema for providing P(VDF-TrFE-CTFE) polymers and members of the EPFL-LMTS for helpful discussions.

Conflict of Interest

The authors declare no conflict of interest.

Keywords

electrostatic clutch, haptic glove, kinesthetic feedback, P(VDF-TrFE-CTFE), wearables textile integration

Received: October 7, 2019

Revised: November 25, 2019

Published online: December 18, 2019

- [1] D. Rus, M. T. Tolley, *Nature* **2015**, 521, 467.
- [2] P. Polygerinos, N. Correll, S. A. Morin, B. Mosadegh, C. D. Onal, K. Petersen, M. Cianchetti, M. T. Tolley, R. F. Shepherd, *Adv. Eng. Mater.* **2017**, 19, 1700016.
- [3] J. Shintake, V. Cacucciolo, D. Floreano, H. Shea, *Adv. Mater.* **2018**, 30, 1707035.
- [4] S. I. Rich, R. J. Wood, C. Majidi, *Nat. Electron.* **2018**, 1, 102.
- [5] L. Hines, K. Petersen, G. Z. Lum, M. Sitti, *Adv. Mater.* **2017**, 29, 1603483.
- [6] S. H. Collins, M. Bruce Wiggin, G. S. Sawicki, *Nature* **2015**, 522, 212.
- [7] C. J. Walsh, K. Endo, H. Herr, *Int. J. Humanoid Rob.* **2007**, 04, 487.
- [8] S. Diller, C. Majidi, S. H. Collins, in *2016 IEEE Int. Conf. Robot. Autom.*, IEEE, Stockholm, Sweden **2016**, pp. 682–689.
- [9] R. Hinchet, V. Vechev, H. Shea, O. Hilliges, in *31st Annu. ACM Symp. User Interface Softw. Technol. - UIST'18*, ACM Press, Berlin, Germany **2018**, pp. 901–912.
- [10] I. Zubrycki, G. Granasik, *J. Intell. Rob. Syst.* **2017**, 85, 413.
- [11] X. Gu, Y. Zhang, W. Sun, Y. Bian, D. Zhou, P. O. Kristensson, in *Proc. 2016 CHI Conf. Hum. Factors Comput. Syst. - CHI'16*, ACM Press, San Jose, California, USA **2016**, pp. 1991–1995.
- [12] T. Yakimovich, E. D. Lemaire, J. Kofman, *J. Rehabil. Res. Dev.* **2009**, 46, 257.
- [13] J. H. Shin, M. Y. Kim, J. Y. Lee, Y. J. Jeon, S. Kim, S. Lee, B. Seo, Y. Choi, *J. Neuroeng. Rehabil.* **2016**, 13, 17.
- [14] P. Cherelle, V. Grosu, L. Flynn, K. Junius, M. Moltedo, B. Vanderborght, D. Lefeber, *Rob. Auton. Syst.* **2017**, 91, 327.
- [15] G. Elliott, G. S. Sawicki, A. Marecki, H. Herr, in *2013 IEEE 13th Int. Conf. Rehabil. Robot.*, IEEE, Seattle, Washington, USA **2013**, pp. 1–6.
- [16] M. Plooi, G. Mathijssen, P. Cherelle, D. Lefeber, B. Vanderborght, *IEEE Rob. Automation Mag.* **2015**, 22, 106.
- [17] T. Saito, H. Ikeda, *J. Intell. Mater. Syst. Struct.* **2007**, 18, 1181.
- [18] A. S. Shafer, M. R. Kermani, in *2011 IEEE Int. Conf. Robot. Autom.*, IEEE, Shanghai, China **2011**, pp. 4266–4271.
- [19] D. M. Wang, Y. F. Hou, Z. Z. Tian, *Smart Mater. Struct.* **2013**, 22, 025019.
- [20] K. Spanner, B. Koc, *Actuators* **2016**, 5, 6.
- [21] S. B. Diller, S. H. Collins, C. Majidi, *J. Intell. Mater. Syst. Struct.* **2018**, 29, 3804.
- [22] V. Ramachandran, J. Shintake, D. Floreano, *Adv. Mater. Technol.* **2019**, 4, 1800313.
- [23] T. Wang, J. Zhang, Y. Li, J. Hong, M. Y. Wang, *IEEE/ASME Trans. Mechatronics* **2019**, 24, 424.
- [24] M. E. Karagozler, J. D. Campbell, G. K. Fedder, S. C. Goldstein, M. P. Weller, B. W. Yoon, in *2007 IEEE/RSJ Int. Conf. Intell. Robot. Syst.*, IEEE, San Diego, California, USA **2007**, pp. 2779–2786.
- [25] A. Johnsen, K. Rahbek, *J. Inst. Electr. Eng.* **1923**, 61, 713.
- [26] T. Niino, S. Egawa, T. Higuchi, in *[1993] Proc. IEEE Micro Electro Mech. Syst.*, IEEE, Fort Lauderdale, Florida, USA **1993**, pp. 236–241.
- [27] T. Niino, S. Egawa, N. Nishiguchi, T. Higuchi, in *[1992] Proc. IEEE Micro Electro Mech. Syst.*, IEEE, Travemunde, Germany **1992**, pp. 122–127.
- [28] W. M. Zhang, H. Yan, Z. K. Peng, G. Meng, *Sens. Actuators, A* **2014**, 214, 187.
- [29] W. H. Lin, Y. P. Zhao, *Int. J. Nonlinear Sci. Numer. Simul.* **2008**, 9, 175.
- [30] Y. Mafinejad, A. Kouzani, K. Mafinezhad, *Informacije MIDEM* **2013**, 43, 85.
- [31] R. C. Batra, M. Porfiri, D. Spinello, *Smart Mater. Struct.* **2007**, 16, R23.
- [32] H. Imamura, K. Kadooka, M. Taya, *Soft Matter* **2017**, 13, 3440.
- [33] M. Taghavi, T. Helps, J. Rossiter, *Sci. Rob.* **2018**, 3, eaau9795.
- [34] T. Watanabe, T. Kitabayashi, C. Nakayama, *Jpn. J. Appl. Phys.* **1993**, 32, 864.
- [35] T. Nakamura, A. Yamamoto, *ROBOMECH J.* **2017**, 4, 18.
- [36] B. N. J. Persson, *J. Chem. Phys.* **2018**, 148, 144701.
- [37] A. S. Chen, S. Bergbreiter, *Smart Mater. Struct.* **2017**, 26, 025028.
- [38] P. Jain, E. J. Rymaszewski, *IEEE Trans. Adv. Packag.* **2002**, 25, 454.
- [39] P. Jain, E. J. Rymaszewski, *Thin-Film Capacitors for Packaged Electronics*, Springer US, Boston, MA, **2004**.
- [40] I. Choi, N. Corson, L. Peiros, E. W. Hawkes, S. Keller, S. Follmer, *IEEE Rob. Autom. Lett.* **2018**, 3, 450.
- [41] S. Qin, S. Ma, S. A. Boggs, in *Conf. Rec. IEEE Int. Symp. Electr. Insul.*, IEEE, **2012**, pp. 592–595.
- [42] S. Ahmed, Z. Ounaies, M. T. Lanagan, *Smart Mater. Struct.* **2017**, 26, 105024.
- [43] J. H. Tortai, A. Denat, N. Bonifaci, *J. Electrostat.* **2001**, 53, 159.
- [44] F. Paschen, *Ann. Phys.* **1889**, 273, 69.
- [45] R. Tirumala, D. B. Go, *Appl. Phys. Lett.* **2010**, 97, 151502.
- [46] F. W. Strong, J. L. Skinner, P. M. Dentinger, N. C. Tien, in *Reliab. Packag. Testing, Charact. MEMS/MOEMS V* (Eds: D. M. Tanner, R. Ramesham), **2006**, p. 611103.
- [47] M. D. Bartlett, A. B. Croll, D. R. King, B. M. Paret, D. J. Irschick, A. J. Crosby, *Adv. Mater.* **2012**, 24, 1078.
- [48] M. D. Bartlett, A. J. Crosby, *Langmuir* **2013**, 29, 11022.
- [49] K. C. Kao, in *Dielectr. Phenom. Solids*, Elsevier, **2004**, pp. 41–114.
- [50] J. Guo, T. Bamber, M. Chamberlain, L. Justham, M. Jackson, *J. Phys. D: Appl. Phys.* **2016**, 49, 415304.
- [51] G. G. Raju, in *Dielectr. Electr. Fields*, CRC Press, **2016**, p. 796.
- [52] L. A. Dissado, J. C. Fothergill, *Electrical Degradation and Breakdown in Polymers*, IET, London, UK **1992**.
- [53] C. Cao, X. Gao, J. Guo, A. Conn, *Appl. Sci.* **2019**, 9, 2796.
- [54] C. Pacchierotti, S. Sinclair, M. Solazzi, A. Frisoli, V. Hayward, D. Prattichizzo, *IEEE Trans. Haptics* **2017**, 10, 580.
- [55] D. Prattichizzo, F. Chinello, C. Pacchierotti, M. Malvezzi, *IEEE Trans. Haptics* **2013**, 6, 506.
- [56] H. Culbertson, S. B. Schorr, A. M. Okamura, *Annu. Rev. Ctrl., Rob., Auton. Syst.* **2018**, 1, 385.
- [57] J. Perret, E. B. Vander Poorten, in *ACTUATOR 2018; 16th Int. Conf. New Actuators*, VDE, Bremen, Germany **2018**, pp. 1–5.
- [58] M. Sreelakshmi, T. D. Subash, *Mater. Today: Proc.* **2017**, 4, 4182.
- [59] A. El Saddik, *IEEE Instrum. Measurement Mag.* **2007**, 10, 10.
- [60] M. A. Eid, H. Al Osman, *IEEE Access* **2016**, 4, 26.
- [61] S. Schlatter, P. Illenberger, S. Rosset, *HardwareX* **2018**, 4, e00039.